Neuron, Vol. 37, 85–97, January 9, 2003, Copyright ©2003 by Cell Press

A Fluorometric Approach to Local Electric Field Measurements in a Voltage-Gated Ion Channel

Osei Kwame Asamoah,[1] Joseph P. Wuskell,[2] Leslie M. Loew,[2] and Francisco Bezanilla[1,*]
[1]Department of Physiology
Department of Anesthesiology
David Geffen School of Medicine
University of California, Los Angeles
Los Angeles, California 90095
[2]Department of Physiology
Center for Biomedical Imaging Technology
University of Connecticut Health Center
Farmington, Connecticut 06030

Summary

Site-specific electrostatic measurements have been limited to soluble proteins purified for in vitro spectroscopic characterization or proteins of known structure; however, comparable measurements have not been made for functional membrane bound proteins. Here, using an electrochromic fluorophore, we describe a method to monitor localized electric field changes in a voltage-gated potassium channel. By coupling the novel probe Di-1-ANEPIA to cysteines in Shaker and tracking field-induced optical changes, in vivo electrostatic measurements were recorded with submillisecond resolution. This technique reports dynamic changes in the electric field during the gating process and elucidates the electric field profile within Shaker. The extension of this method to other membrane bound proteins, including transporters, will yield insight into the role of electrical forces on protein function.

Introduction

Electrical signals in the nervous system are generated by the activity of a superfamily of integral-membrane proteins known as voltage-dependent ion channels. These proteins reside in a complex electrostatic environment that is established by the interaction of multiple charged species, both intrinsic and extrinsic to the protein (Green and Andersen, 1991), in the context of a complex protein molecular surface (Honig and Nicholls, 1995). The functional implications of electrostatics on ionic conduction (Hille et al., 1975; Ohmori and Yoshii, 1977) and voltage sensitivity (Hodgkin and Huxley, 1952) have been long recognized. However, dynamic measurements of electric field changes within a channel have not yet been achieved. Consequently, the role that ion channel structure serves in "tuning" the electrical forces responsible for voltage sensor movement remains unknown.

Although theoretical approaches to protein electrostatics have proven exceptionally informative when applied to soluble molecules, these techniques have only been of limited utility when applied to integral-membrane proteins. Classical electrostatic methodologies rely on high-resolution structural data to generate detailed surface potential profiles. As an atomic-resolution structure for an intact voltage-gated ion channel is not available, a thorough mapping of electrostatic interactions onto a voltage-sensor structure has not been realized. Nevertheless, the prospect of ultimately gaining such a definitive view of the voltage-sensor has been heralded with the crystallization of Kcsa, a prokaryotic potassium channel (Doyle et al., 1998). While this immense achievement has elucidated the molecular requirements for high-fidelity ionic conduction, little insight was provided toward the voltage-sensitive properties of ion channels.

Experimental methods that provide direct electrostatic information, without the requirement for precise structural information, suffer from a variety of limitations. For instance, in vitro spectroscopic techniques, including NMR and IR spectroscopy, require relatively large quantities of soluble protein. Furthermore, in the case of NMR, the time scale of this method is too slow to track electrical changes coupled to fast gating transitions. In other methods, such as cyclic voltammetry and pH shift analysis, the identification of the redox or acidic group involved in the electrostatic interaction is complicated when multiple species are present within the protein. Recent advances in atomic force microscopy (AFM), on the other hand, have provided high spatial resolution surface potential images of a bacterial channel (Philippsen et al., 2002). Although this technique demonstrates exquisite sensitivity in detecting electrostatic perturbations, at present, AFM is of limited applicability due to the need for protein reconstitution into lipid bilayers.

In this communication, we describe the use of a cysteine-reactive electrochromic fluorophore to track spatially localized electrostatics in the Shaker potassium ion channel. The functional unit of the K^+ channel is a homotetramer with each subunit consisting of six putative membrane spanning segments (S1–S6) (Figure 2A). The fourth transmembrane segment (S4) is regarded as the primary voltage sensor, in part due to its characteristic primary sequence in which every third amino acid is a cationic residue (arginine or lysine), while the intervening residues are hydrophobic. With this novel fluorometric technique, we show that the electric field in an extracellular domain decreases as the channel gates from the closed to open state. As evidence of the sensitivity of our technique, we demonstrate that the electric field within the protein matrix is modulated by changes in extracellular calcium and pH. Finally, we reveal for the first time that an electric field gradient exists in Shaker (see Figure 2A for the approximate location of the following residues) with a minimal field near the N terminus of the S3-S4 extracellular linker (residue 345C) and progressively larger electrostatic field strengths measured near C-terminal residues (354C, 359C) of this region. While significant field strengths are found both within the S3-S4 linker (359C) and the pore (425C), the maximal electrostatic potential is measured near the second gat-

*Correspondence: fbezanil@ucla.edu

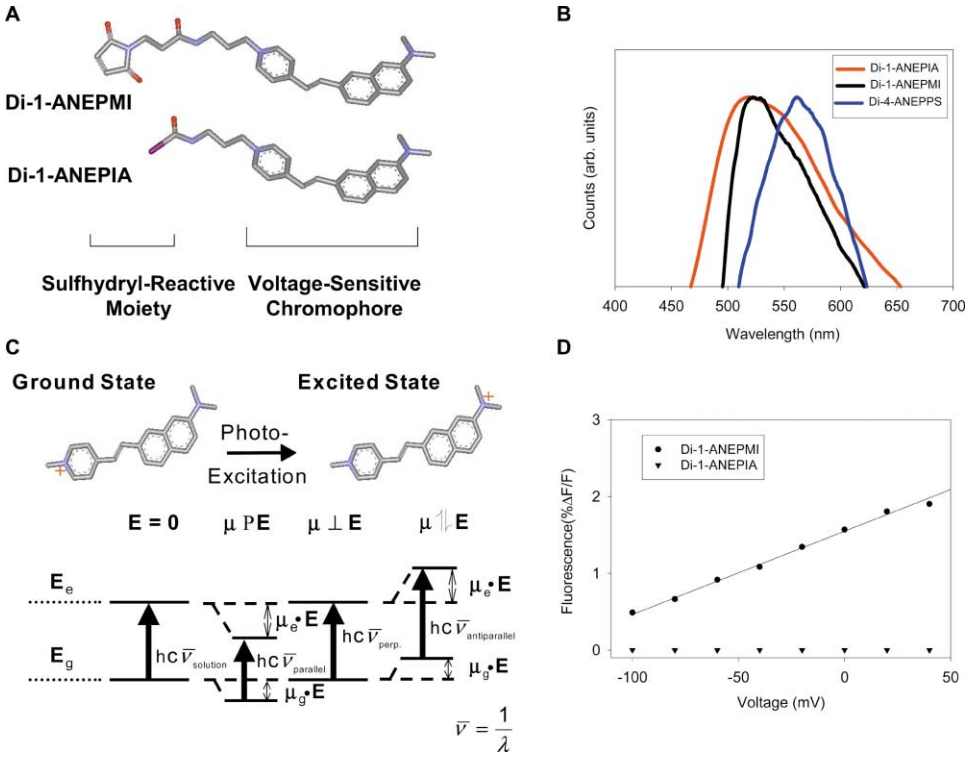

Figure 1. Structure and Properties of Cysteine-Reactive Electrochromic Fluorophores

(A) Structure of Di-1-ANEPMI (top) and Di-1-ANEPIA (bottom).

(B) The fluorescence emission spectra of Di-1-ANEPMI (black), Di-1-ANEPIA (orange), and Di-4-ANEPPS (blue). These spectra are not corrected for the wavelength dependence of the detector.

(C) The molecular basis of the electrochromic process is depicted at the top. The perturbation of the electronic energy levels in the presence of an electric field produces a shift in the fluorescence spectra that is manifested as a rapid optical signal. P indicates a parallel orientation.

(D) Evoked fluorescence from *Xenopus* oocytes expressing the cysteine-less Shaker mutant W434F. The cells were stained in 5 μM Di-1-ANEPMI or an equivalent concentration of Di-1-ANEPIA, then voltage clamped to the indicated potentials.

ing charge (365C) in the fourth transmembrane segment (S4). This result provides direct heuristic evidence of an amplified electric field in the region through which gating charges translocate.

Results

Characterization of a Unique Class of Electrochromic Dyes

To map the electric field profile along the Shaker channel, a novel class of potentiometric dyes was developed. These fluorophores are comprised of two functional domains (see Figure 1A): the ANEP chromophore that has proven to be a sensitive molecular indicator of transmembrane electrical events (Zhang et al., 1998) and a sulfhydryl-reactive moiety to which cysteine residues covalently bind. Efficient yet specific fluorophore attachment is critical to realizing site-specific electrostatic recordings in channels. Consequently, two reagents with different thiol-reactive groups were screened for their suitability. 1-[3-(β-Maleimidopropionyl) aminopropyl]-4-[β-[2-(dimethylamino)-6-naphthyl] vinyl] pyridinium bromide (referred to as Di-1-ANEPMI) contains a maleimide ring (Figure 1A, top), while 1-[3-(Iodoacetyl) amino propyl]-4-[β-(2-dimethylamino)-6-naphthyl] vinyl pyridinium bromide (or Di-1-ANEPIA) employs an iodoacetamide moiety (Figure 1A, bottom) to form stable protein-dye adducts. An important consideration for both dyes was to distinguish ion channel labeling from nonspecific labeling of the plasma membrane. To distinguish between these possibilities, we have exploited the environmental sensitivity of fluorescence emission spectroscopy (Lakowicz, 1999). The emission spectra of both thiol-reactive fluorophores, when bound to Shaker channels expressed in *Xenopus* oocytes, suggest that they reside in comparable environments (Figure 1B, red and black traces). However, in the same membranes, the spectra of the electrochromic probe Di-4-ANEPPS, which contains the same chromophore but is designed to partition into membranes, is shifted, suggesting that this probe samples a different environment (Figure 1B, blue trace).

The voltage-sensitive properties of the ANEP chromophore are derived from a photoexcitation-induced process (Figure 1C, top; Loew, 1982). Upon illumination, the cationic charge localized on the pyridinium nitrogen shifts to the aminonaphthyl group, causing a change in the molecule's dipole moment. This differential dipole moment $\vec{\mu}_g - \vec{\mu}_e$ couples to the local electric field and perturbs the electronic energy levels of the ground and excited state (Figure 1C, bottom). Consequently, the

electrochromic effect is manifested as a spectral shift as described by the following equation (Loew et al., 1978):

$$hc\Delta\bar{\nu} = (\vec{\mu}_g - \vec{\mu}_e) \cdot \vec{E}, \quad (1)$$

where $\Delta\bar{\nu}$ is the spectral shift (in reciprocal wavelength) induced by the effective field strength, $\vec{E}$, c is the speed of light (3×10^8 m/s), and $\vec{\mu}_g$ and $\vec{\mu}_e$ represent the ground and excited state dipole moments, respectively.

As the spectral shifts expected with physiologically relevant electric field strengths are extremely small in magnitude (Loew, 1982), we monitor changes in fluorescence intensity that are induced by the voltage-dependent spectral shifts. In this scenario, membrane voltage simply shifts the excitation and emission spectra relative to fixed bandwidth filters and produces a change in both the proportion of fluorophores excited and in the collection efficiency of the system. In the limit of small spectral shifts, the linear dependence of the spectral shift with voltage is manifested as a linear change in the detected fluorescence intensity with membrane voltage (see section entitled Calibration of Di-1-ANEPIA Fluorescence Sensitivity Relative to Di-4-ANEPPS in Experimental Procedures).

Reliable electric field measurements within the channel require the suppression of a variety of nonspecific optical signals. In particular, dye molecules that partition into the cell membrane or bind to a variety of integral membrane proteins may detect changes in the transmembrane electric field and generate noise. To evaluate the specificity of the electrochromic signals, we stained *Xenopus* oocytes expressing the nonconducting Shaker mutant W434F in a 5 μM solution of Di-1-ANEPMI or Di-1-ANEPIA. Since this channel mutant does not contain external cysteine residues, any voltage-dependent fluorescence signal represents the nonspecific population of fluorophores in our system. Voltage-clamp experiments demonstrate that oocytes stained with Di-1-ANEPMI exhibit linear ($r^2 = 0.996$) voltage-dependent fluorescence signals (Figure 1D, circles) across the tested voltage regime. In contrast, cells exposed to Di-1-ANEPIA for an equivalent staining period do not exhibit an optical signal (Figure 1D, inverted triangles).

Fast Optical Signals Accompany Voltage Changes in Shaker

The data presented above indicate that Di-1-ANEPIA may be exploited as a site-specific electric field probe in Shaker due to its intrinsic insensitivity to changes in membrane voltage. To assess this possibility, we coupled Di-1-ANEPIA to a cysteine residue (354C) in the S3-S4 extracellular linker of Shaker. A voltage step to -60 mV (Figure 2B, top) elicited a gating current (same figure, middle) representative of the W434F mutants (Perozo et al., 1993) and a robust fluorescence change (Figure 2B, bottom). This optical signal was comprised of two distinct kinetic components: a fast "jump" coincident with the change in command voltage, and slower fluorescence signals that followed. To further explore the relationship between the applied voltage and fluorescence, a large membrane depolarization to 40 mV (Figure 2C, top) was given. As expected, a larger gating current was elicited (Figure 2C, middle), while the optical signal exhibited additional complexity. At this potential, the first component remains extremely fast and increases in magnitude (Figure 2C, bottom). However, the slower fluorescence component is not only modified in time course, but exhibits a reversed orientation. The fluorescence "jumps" are indicative of electrochromic phenomena, as the fast kinetics are voltage-independent while the magnitudes scale with the command potential. For this reason, the transition observed at the instant of membrane depolarization is designated the Electrochromic On (Eon) (Figure 2D, insert) and the signal observed upon repolarization is termed the electrochromic off (Eoff) (Figure 2D, insert), with the on and off denoting the depolarizing and hyperpolarizing voltage transition, respectively. While the molecular basis for these fast signals reflect the chromophore's voltage-sensitive attributes, the precise origin of the slow component is less clear. Significant environmental changes within the protein matrix accompany gating events (Cha and Bezanilla, 1997; Mannuzzu et al., 1996) and may alter the quantum yield of the fluorophore. Alternatively, conformational transitions of Shaker could merely facilitate dye reorientation and generate a slow electrochromic signal as the dipole moment of Di-1-ANEPIA changes relative to the transmembrane electric field direction (see Equation 1). The underpinnings of this slow fluorescence component is explored below.

The Voltage Dependence of the Electrochromic Signals Reflect Electrostatic Properties

Consistent with our primary goal of elucidating protein electrostatics, we sought a quantitative measure of local field strengths at different regions of the channel. The ANEP chromophore exhibits linear voltage-dependent behavior (Loew et al., 1992) in diverse preparations. As this linear behavior ensures an optical response that is proportional to the field magnitude, the slope of the fluorescence-voltage relation, in fact, reflects the localized electric field strength. The normalized change in fluorescence (% dF/F) of Eon (circles) and Eoff (upright triangles) components are plotted as a function of test potential for site 354C (Figure 2D, large figure). The line at zero serves as a visual cue to emphasize the opposing direction of the two electrochromic signals. Since the electrochromic on signal is concomitant with membrane depolarization (see Figures 2B and 2C), the fluorescence at this instant of time represents the closed state of the channel (see below). The conditioning pulse to -90 mV ensures that the protein begins in the same initial condition, or conformational state, regardless of the applied test potential. Consequently, the ANEP chromophore essentially resides in a quasistatic environment of increasing field strength at the time at which the electrochromic on signal is recorded. This is the molecular basis for Di-1-ANEPIA's linear voltage response ($r^2 = 0.994$). Unlike Eon, the magnitude of the electrochromic off is not strictly proportional with voltage (Figure 2D, upright triangles). This signal is recorded 60 ms after the depolarizing stimulus, and therefore reflects the electric field of the ensemble of channel structures available at each test voltage.

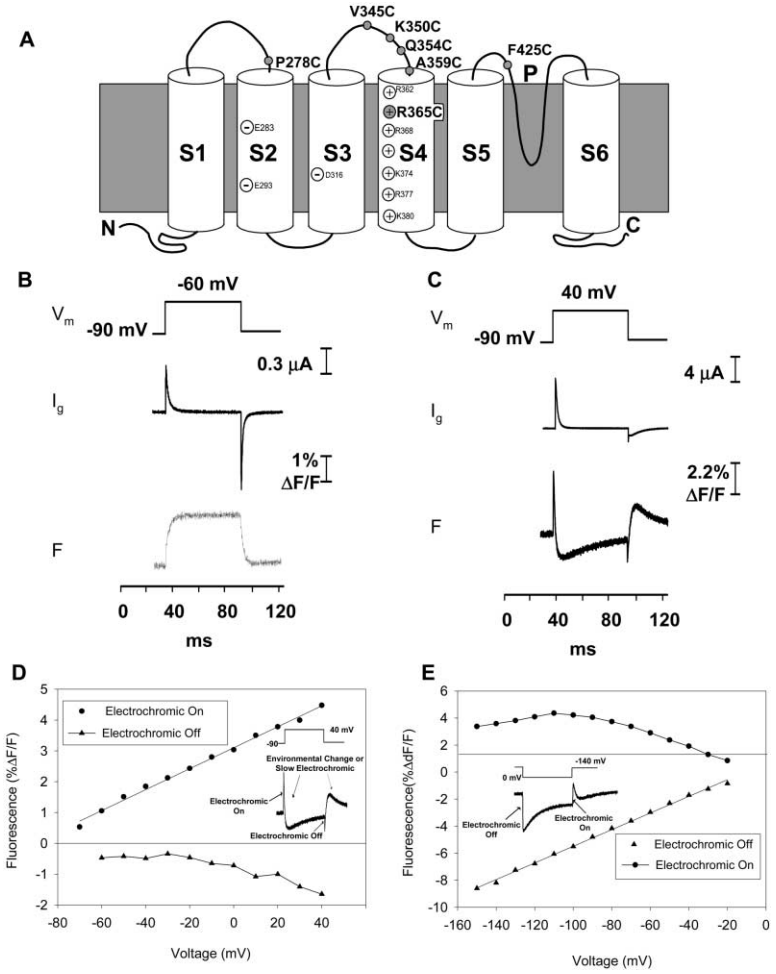

Figure 2. Optical Signals of Di-1-ANEPIA in the S3-S4 Linker (Residue 354C) and Near the S4 Segment (Residue 359C) of Shaker

(A) The basic subunit of Shaker is depicted with the approximate locations of the cysteine residues in which the electrostatic field was measured.

(B and C) *Xenopus* oocytes expressing a Shaker mutant with an introduced cysteine residue (354C) in the S3-S4 linker exhibit gating currents (I_g) and fluorescence signals (F) with depolarizing pulses to −60 mV (B) and 40 mV (C).

(D) The magnitude of the electrochromic signals are plotted as a function of voltage to quantitate the electrostatic field at site 354C. The electrochromic on (circles) is linear (r^2 = 0.994) with voltage while the electrochromic off (inverted triangles) is highly nonlinear. Inset: the evoked fluorescence with a depolarization pulse to 40 mV.

(E) The electrochromic off (inverted triangles) exhibits linear voltage dependence (r^2 = 0.997), while the electrochromic on (circles) is nonlinear with voltage with this pulse protocol. Inset: fluorescence response to voltage pulses from the activated state (0 mV) at site 359C. Eon is designated by the leftward arrow and Eoff denoted by rightward arrow.

Assuming our hypothesis concerning the linear voltage-dependence of the Eon is correct, the electrochromic off signal will also exhibit linear behavior with the proper experimental conditions. Specifically, by biasing the channel in the activated state with a positive holding potential, hyperpolarizing test pulses should elicit linear voltage-dependent Eoff signals. We tested this idea by probing the extracellular region of the voltage sensor at residue 359C. To be consistent with our earlier convention, the large fluorescence signal evoked by membrane hyperpolarization (Figure 2E, inset) was designated the electrochromic off, while the rapid optical component noted upon returning to 0 mV was denoted the electrochromic on (same inset). Here the magnitude of Eon was biphasic with voltage (circles in Figure 2E, large figure) and, as predicted, the electrochromic off signal (upright triangles of same figure) exhibited linear voltage-dependent behavior (r^2 = 0.997).

Although the coincidence of Eon and the command pulse suggests that this optical signal is electrochromic in nature, a kinetic analysis was employed to substantiate this mechanism. As shown in Figure 3A, the Eon (indicated by the arrowhead) at site 354C superimposes with the capacitance charge (red trace). Accordingly, this fast optical signal occurs at the same time scale at which the voltage is established across the membrane. Moreover, average voltage sensor movement, as represented by gating charge displacement (blue trace), is significantly slower than the electrochromic on. This large discrepancy in kinetics substantiates that Eon represents the electrostatics of the channel preceding major gating transitions. Conversely, the slow fluorescence component (decaying portion of black trace) and gating charge (blue trace) are kinetic correlates. This is better illustrated in Figure 3B where the time constant of gating charge (red) and fluorescence (black) are comparable between −10 mV and 40 mV.

Optical changes of dye-labeled residues near the S4 segment are known to reflect conformational changes associated with movement of the voltage sensor (Baker et al., 1998; Sorensen et al., 2000). Thus, the kinetic correspondence between the slow fluorescence and gating charge movement is not surprising. However, unlike Di-1-ANEPIA, the fluorescent probes utilized to date report environmental changes in the vicinity of the S4 (Cha and Bezanilla, 1998) rather than protein electrostatics. To determine whether the slow fluorescence component at residue 354C reflects a slow electrochromic process due to fluorophore reorientation or a simple environmental change, a variable duration test pulse protocol was utilized (Figure 3C, top). The time course of electric field modulation is determined by comparing Eon (Figure 3C, rightward directed arrow) and Eoff (same figure, leftward directed arrow) at various

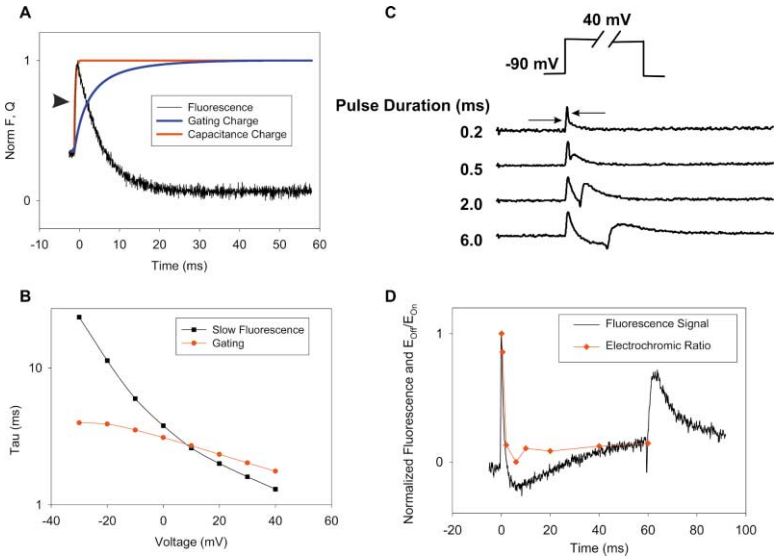

Figure 3. Temporal Response of the Cysteine-Reactive Electrochromic Probe

(A) The electrochromic on signal (arrowhead pointing to upward deflection of black trace), capacity charge (orange), and gating charge (blue) at site 354C (pulse to 40 mV, from a holding potential of −90 mV).

(B) The time constants of the slow fluorescence (black squares) and gating charge (red circles).

(C) The kinetics of electric field modulation during the gating process assayed by comparing the magnitude of the electrochromic on (rightward arrow) and electrochromic off (leftward arrow) as a function of pulse duration at 40 mV.

(D) A time plot of the normalized electrochromic ratio (red trace) and slow fluorescence (black trace).

times during the gating process. Figure 3D presents the normalized Eoff:Eon ratio superimposed on the raw fluorescence signal recorded with a test pulse to 40 mV. The correlation between the decaying fluorescence component (black trace) and the changing electric field strength (red) indicates that the slow optical signal also reports electrostatic changes. As suggested above, this electrical modulation may be coupled to voltage sensor movement via fluorophore reorientation. However, the subsequent deviation between the electrochromic ratio and the raw fluorescence after a brief time period likely reflects environmental changes of Di-1-ANEPIA. Collectively, these observations reveal the bifunctionality of Di-1-ANEPIA as both an electrostatic reporter and probe of environmental changes.

Protein Electrostatics Are Sensitive to Variations in Extracellular Calcium and Hydrogen Ion Concentration

Next, we examined the sensitivity of the localized electric field to ionic perturbations. This measure is particularly relevant near the S4 segment where electrical events are transduced into conformational changes (Cha et al., 1999; Glauner et al., 1999). For this purpose, we compared the slope of the electrochromic off signals in 0.5 mM and 70 mM extracellular calcium solutions (see Table 1 for solution composition and properties) at site 359C. Calcium ions influence protein electrostatics by screening fixed surface charges (σ_T) (Ji et al., 1993) and modulating the debye length (κ^{-1}) of the surrounding solution (Islas and Sigworth, 2001). Thus, the net effect of elevated calcium is to attenuate the electrostatic field at the protein-solution interface and the component of the transmembrane potential that extends into the solution. As shown in Figure 4A, high calcium (square symbols) shifted gating charge in a depolarized direction relative to low calcium (inverted triangles), indicative of its membrane stabilizing effect (Brink, 1954). The shift of $+22.1 \pm .04$ mV (mean ± SEM, n = 6) of the gating charge is a direct consequence of an attenuated surface potential (ψ_0) (as determined from Equation 2) in the presence of high calcium concentration. In addition to modulating ion channel gating, elevated calcium diminished the electric field strength by 18.8% ± 3.9% (four different oocytes), as indicated by the decreased slope of the electrochromic off (Figure 4B, square symbols). The basis of the electrostatic field reduction may reflect the decreased surface potential of Shaker, the attenuated debye length in solution (Table 1), or a combination of the two effects. To better understand the contribution of each toward modifying the electric field, we exploited the effect of hydrogen ions on ion channel gating. Variations in extracellular proton concentration modulate surface charge density, yet maintain the debye length at a fixed value (Table 1). Unlike the screening effect of calcium ions, protons associate with acidic groups on the protein surface, essentially neutralizing fixed charges. Thus, decreasing the pH from 7.4 to 5.5 displaced voltage sensor movement by $+21.7 \pm 4.7$ mV (n = 6) (Figure 4C), consistent with a decreased surface potential previously reported (Starace et al., 1997). As illustrated in Figure 4D, the localized electric field was diminished to a greater extent (30.3% ± 5.4%, four oocytes) by the increased proton concentration relative to elevated calcium. This robust effect of pH on protein electrostatics reflects proton binding with a pK_a of 4.59 (equation 5) of Shaker. Similar pK_a values have been reported for other voltage-dependent channels (Hille et al., 1975; Ohmori and Yoshii, 1977). Accordingly, the electric field strength at the extracellular portion of the S4 is very sensitive to changes in the surface potential, but not

Table 1. Composition and Debye Length of Extracellular Solutions

Solutions	NMG-Mes	HEPES	$CaCl_2$	$Ca(Mes)_2$	MES	pH	κ^{-1} (A)
NMG-0.5 Ca^{2+}	112	10	0.5			7.4	8.9
NMG-70 Ca^{2+}	10	10		70		7.4	6.5
NMG-pH 7.4	120	10	2			7.4	8.5
NMG-pH 5.5	120		2		10	5.5	8.5

Solutions at pH 7.4, pH 5.5 and solutions of 0.5 Ca^{2+}, 70 Ca^{2+} at 255 mosmolal and 240 mosmolal, respectively.

Mes, Methanesulfonic acid; MES, (2-[N-Morpholino]ethanesulfonic acid).

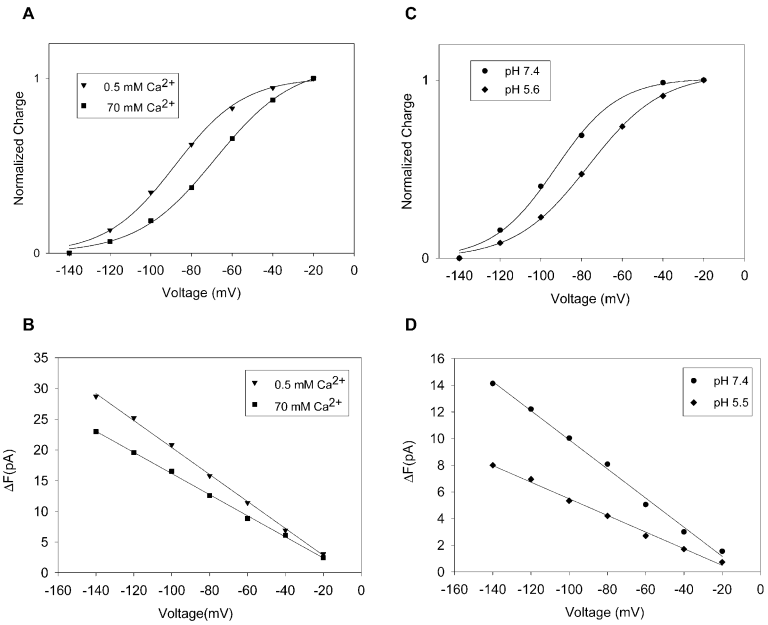

Figure 4. Electric Field Sensitivity of Di-1-ANEPIA in the N Terminus (Residue 359C) of the Fourth Transmembrane Segment

(A) Voltage sensor displacement in 0.5 mM (inverted triangles) versus 70 mM [Ca^{2+}] (squares).

(B) Analysis of the change in the electric field strength for the oocyte shown in (A). The magnitude of the electrochromic off signal (given in units of pA, as recorded by a photodiode coupled to an integrating headstage of a patch-clamp amplifier) in the two extracellular calcium conditions.

(C) Modulation of gating charge movement induced by increased proton concentration in the extracellular solution.

(D) Electrostatic attributes near the S4 are very sensitive to changes in the pH of the extracellular solution with an average field modulation of 30.3% $\pm$ 5.4% (n = 4) observed in acidic conditions.

All of the above data were obtained with the following voltage pulse protocol: HP = 0 mV, test pulse to indicated value, post-pulse = 0 mV. The off component of the gating current was integrated for (A) and (C) while the electrochromic off fluorescence was utilized for (B) and (D).

the component of the transmembrane electric field that decays in solution. This result indicates that when attached to residue 359C, Di-1-ANEPIA lies in close proximity to the molecular surface of the channel and does not report electrostatic changes in "bulk" solution. This interpretation is supported by a numerical solution to the Poisson-Boltzmann equation (Equation 6), in which the electric field in the aqueous solution is calculated as a function of distance from the Shaker surface. By equating the attenuation of the electrochromic signal measured in high versus low extracellular calcium (18.8%) to the calculated difference values obtained in these two ionic conditions, we determined that Di-1-ANEPIA lies approximates 4 Å from the center of mass of Shaker surface charge density. While the use of the one-dimensional Poisson-Boltzmann equation is clearly an oversimplification of a three-dimensional problem, our lack of structural information justifies its use. Consequently, our calculation is only an approximation, though it is noteworthy that a similar distance (5 Å) was reported between a MTS reagent bound to the S4 and an electrostatically coupled glutamate residue in the S5-S6 loop (Elinder and Arhem, 1999).

The Transmembrane Electric Field Is Maximized in the Voltage Sensor

Starting from the extracellular side, the first four arginines in the fourth transmembrane segment are the primary gating charges in the Shaker potassium channel (Aggarwal and MacKinnon, 1996; Seoh et al., 1996). These residues move from a narrow aqueous crevice (Bezanilla, 2000) continuous with the intracellular compartment to a different crevice exposed to the extracellular milieu (Starace and Bezanilla, 2001). We evaluated the electric field strength in the voltage sensor by attaching Di-1-ANEPIA to residue 365C (the second charge of the S4 segment). The electrochromic response at this site was unique in a number of ways. First, as depicted in the lower trace of Figure 5A, the electrochromic on and off at this position were inverted with respect to the signals recorded in the S3-S4 linker (refer to Figures 2B and 2C) and all other sites probed in the channel. Consequently, Di-1-ANEPIA must orient in the reverse direction at this location, presumably due to steric constraints within this region of the voltage sensor (Larsson et al., 1996). It is noteworthy that the detected field diminished at large applied voltages (see upper trace of Figure 5A), implying that the potential gradient has been "focused" (Starace et al., 1997) away from the chromophore. Thus, in contrast to the other sites that were probed, Eon in R365C exhibited nonlinear voltage dependence (circles in Figure 5B) from the closed state (i.e., prepulse of -90 mV) likely due to fast reorientation of proximal side chains during the voltage transition or a change in the angle of the fluorophore.

To quantitate the electrostatics that operate on gating charge movement in the S4 and to assess the field properties along the Shaker structure, we translated the electrochromic measurements into standard units of electric field strength. The fluorescence from a standard potentiometric reagent was utilized to calibrate the in vitro optical signal. *Xenopus* oocytes devoid of channels were stained with Di-4-ANEPPS and the slope of the fluorescence-voltage relation was established (data not shown). This parameter was subsequently converted to an electric field measure by assuming a membrane thickness of 30 Å. In this manner, the voltage sensitivity (or slope) of Di-4-ANEPPS was directly equated to the magnitude of the electric field. Before the calibration was applied to the signals from Shaker, a correction factor was required. Electrochromic-based fluorescence signals arise from the relative change in the illuminated area under the excitation spectrum and the change in detection area under the emission spectra that occur

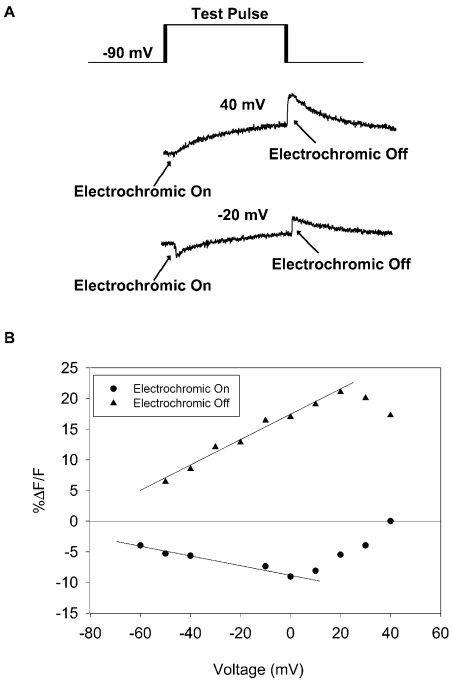

Figure 5. The Electrochromic Signals in the S4 Has Unique Attributes

(A) The rapid optical signals at site 365C exhibit an inverted orientation (relative to all other sites) such that the electrochromic on (right arrow) and electrochromic off (left arrow) are downward and upward, respectively.

(B) The electrochromic on (circles) in the S4 demonstrates nonlinear voltage dependent behavior with an electric field sensitivity (slope) that is significantly attenuated with respect to the electrochromic off (inverted triangles).

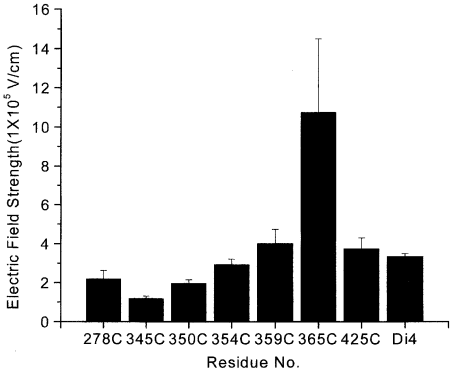

Figure 6. The Electrostatic Field in Shaker Is Maximized in the Fourth Transmembrane Segment

The electrostatic field profile in Shaker as determined from the average slope of the fluorescence versus voltage relationship measured at each site. The electrochromic on fluorescence signal was utilized for all residues with the exception of 365C, for which the electrochromic off was employed. In all cases, a voltage pulse protocol with HP = −90 mV, variable amplitude test pulse from −140 mV to 40 mV in increments of 20 mV, and a return pulse to −90 mV was used. The electric field strength in the protein was calculated using Di-4-ANEPPS as a calibration reference (see Experimental Procedures).

with spectral shifts. Therefore, to compare the electrochromic sensitivity of Di-1-ANEPIA to Di-4-ANEPPS, the slope of the % *dF/F* versus spectral shift relationship for the excitation (bandpass region between 425 nm and 475 nm utilized for both dyes) and the emission spectra (cut-on wavelength of 515 nm for Di-4-ANEPPS and 565 nm for Di-1-ANEPIA) were calculated (see Calibration of Di-1-ANEPIA Fluorescence Sensitivity Relative to Di-4-ANEPPS in the Experimental Procedures section). Once the relative sensitivity between the two dyes was determined, the electrochromic slope measured at each site in Shaker was converted into an electric field strength. In reality, these values represent a lower limit of the actual electrostatic field as the fluorophore may be tilted away from the normal of the membrane surface (as further discussed below). With this approach, we ascertained that a pronounced electrostatic field gradient exists along the S3-S4 extracellular domain (note residues 345–359 in Figure 6) and culminates in a magnified field strength in the primary voltage sensor (amino acid 365, Figure 6). Furthermore, residue 278, which resides in the extracellular end of the S2 segment, experiences a field strength slightly smaller than that within the bilayer. Finally, we note that an electrostatic field equivalent to that in the membrane but larger than the field near 278C emanates from the outer region of the pore (site 425, Figure 6). It is possible that this field serves as an electrostatic "funnel" for cation delivery to the entrance of the permeation pathway.

In Figure 7A, we present a structural model depicting Di-1-ANEPIA attached to residue 365 of the voltage sensor. The orientation of the fluorophore was inferred from the polarity of the electrochromic signals at this site relative to signals obtained from Di-4-ANEPPS. As the midpoint of the electrochromic charge shift (blue dot) is not adjacent to the fluorophore's site of attachment, it is apparent that an electric field "focused" to a small region near the α-helical backbone may escape detection by the chromophore. A mechanistic interpretation (Figure 7B) for the electrical hysteresis at this site is also offered. In the closed conformation of the voltage sensor (left), gating charges reside in an intracellular crevice (Starace et al., 1997) and thereby result in the convergence of the transmembrane electric field lines. As the fluorophore is restricted to the extracellular face of the S4 and is oriented away from the intracellular crevice, a relatively small electric field is detected at the instant of membrane depolarization (Eon, Figure 5B). However, as the voltage sensor transports gating charge across the hydrophobic membrane core into an external crevice, the electric field density is now localized to the same electrical compartment as the fluorophore. Consequently, Di-1-ANEPIA exhibits a large electrochromic signal (Eoff, Figure 5B) from the open state.

Discussion

In this work, we demonstrate a fluorometric approach to surveying the electrostatic field in an active protein using the cysteine-reactive electrochromic probe Di-1-ANEPIA. The optical signal of Di-1-ANEPIA is dependent on the presence of external cysteine residues in Shaker (Figure 1D); thus, our data was readily separated from

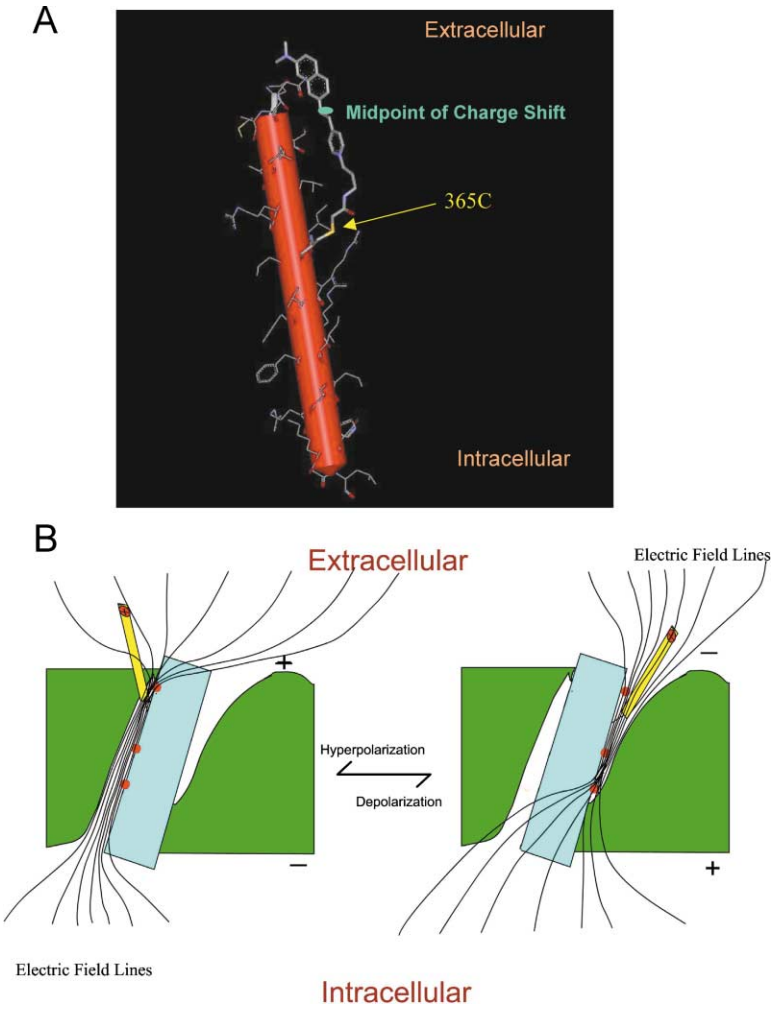

Figure 7. Models of Di-1-ANEPIA Attached to the S4

(A) A structural model depicting Di-1-ANEPIA conjugated to residue 365C. The orientation of the fluorophore was inferred from the polarity of the electrochromic signals recorded in the S4 relative to fluorescence signals observed in oocytes labeled with Di-4-ANEPPS. (B) A mechanistic model illustrating the origin of electrical hysteresis in the voltage sensor.

potential sources of "noise" including membrane-partitioned flurophores and dye molecules bound to other proteins present on the cell surface. In the S3-S4 extracellular linker, we determined strong coupling of the structure-electrostatic relations of Shaker as an attenuating electric field strength correlated with channel gating from closed to open states. Furthermore, we found that the electrical attributes near the fourth transmembrane segment were modulated in a predictable manner by modulation of the ionic strength and pH of the bathing solution. The site-specific nature of our electric field reporter ultimately allowed for the identification of an electric field gradient along Shaker distinguished by an enhanced electrostatic field in the voltage-sensor region.

Di-1-ANEPIA Is a Site-Specific Electric Field Reporter

The electrochromic fluorophore Di-1-ANEPIA was engineered to maximize specificity toward cysteine conjugation in proteins while minimizing associations with the cellular membrane. Toward this aim, it contains an iodoacetamide functional group for thiol reactivity and, in contrast to standard fast potentiometric dyes, only two methyl groups on the anilino nitrogen (Figure 1A) to decrease the hydrophobicity.

Although the decreased reactivity of iodoacetamides relative to maleimides (Meister, 1995) may impede the labeling of cysteine residues, the smaller length of the linker permits electric field detection at regions relatively close to the probe's site of attachment. In fact, the slower reaction rate is likely advantageous in this application as suggested by Di-1-ANEPMI recordings. This maleimide congener produced a significant signal in the absence of external cysteines on Shaker (Figure 1D). This voltage-dependent optical signal likely reflects a large population of intrinsic thiols on the membrane surface that bind to the highly reactive fluorophore and accordingly results in large background fluorescence (data not shown). It is also possible that the nonspecific signal of Di-1-ANEPMI may be independent of thiol reactivity and signify a slightly greater hydrophobicity relative to Di-1-ANEPIA. Consequently, this fluorophore would exhibit more extensive partitioning into the lipid membrane. However, the maleimide derivative is unlikely to interact with the bilayer in a significant manner as inferred by the similarity of Di-1-ANEPIA and Di-1-ANEPMI emission spectra. The fluorescence spectrum

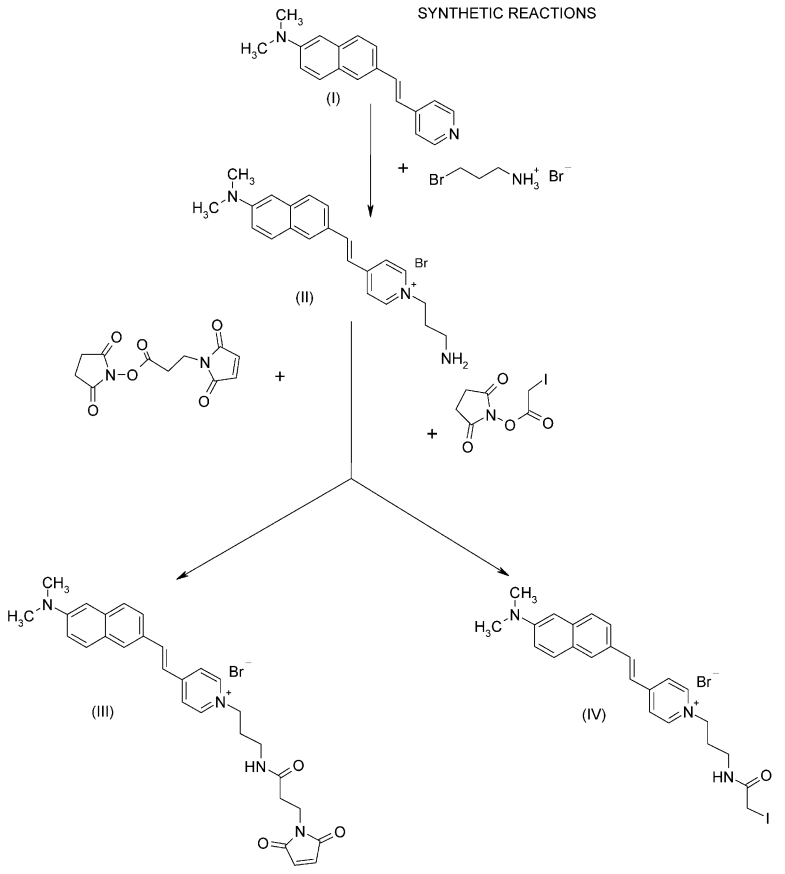

Figure 8. Synthesis of Thiol-Reactive Electrochromic Fluorophores

Di-1-ANEPMI (III) and Di-1-ANEPIA (IV) are synthesized from the precursor β-[2-(Dimethylamino)-6-naphthyl]-4-vinyl pyridine (I).

of a conventional electrochromic probe (Di-4-ANEPPS), on the other hand, exhibited a spectral shift indicative of a distinct molecular environment (Figure 1B). Interestingly, the emission maximum of Di-4-ANEPPS in the oocyte (570 nm) represents a 60 nm "blue shift" relative to that in lipid vesicles (Loew et al., 1992). Although the precise basis for this spectral perturbation is unclear, the heterogeneous lipid and protein composition of the oocyte membrane (Sadler, 2001) likely presents a unique physico-chemical environment as compared to the homogeneous phospholipid vesicle.

Electrostatic Field Description

The utility of fluorescent indicators to report electrical events in biological systems has been recognized for more than 30 years (Carnay and Barry, 1969; Tasaki et al., 1968). Of the various classes of potentiometric dyes (Cohen et al., 1974; Waggoner and Grinvald, 1977) developed for this purpose, electrochromic probes have proven indispensable in elucidating the electrical properties of cells. The advantages of these fluorophores derive from linearity of response and fast kinetics. Because of these attributes, the emitted fluorescence is proportional to the magnitude of the stimulus and is able to faithfully track the time course of electrical fluctuations. Electrochromic dyes have been applied to an extensive range of preparations from isolated cells (Loew et al., 1992; Rohr and Salzberg, 1994) to intact organ systems (Canepari et al., 1996; Yuste et al., 1997). Of particular interest, potentiometric fluorophores have been utilized to resolve gradients of the intramembrane electric field along the surface of a neuroblastoma cell (Bedlack et al., 1994) that induced gating disparities in sodium channels within these regions (Zhang et al., 1996). However, as standard electrochromic probes reside in the lipid bilayer, the electrical potential that directly acts on the voltage-sensing machinery was not accessible. In contrast, the method presented in this paper offers a molecular description of the electrostatics within the protein matrix.

Here, the optical signals generated by Di-1-ANEPIA allowed us to probe the electrical attributes of Shaker with high temporal resolution and in a site-directed manner. The field within the ion channel, as exemplified by the electrochromic response in the S3-S4 domain (Figure 2D, large figure), was shown to undergo electrical hysteresis such that a significant electrical force was present in the closed state but a diminished field was experienced from open states. We are confident in this interpretation as the two electrochromic signals exhibit opposite orientations (Eon is upward and Eoff is downward), indicating that the hysteresis could not be attributed to "flipping" of the Di-1-ANEPIA under the influence of voltage.

Our electrostatic description relies on the proper assignment of Eon and Eoff as electrochromic in nature. These assignments were based on the following criteria: (1) the coincidence of both signals with voltage transitions (e.g., Figure 2B); (2) fast kinetics that were independent of the command potential (compare Figures 2B

and 2C); and (3) in the case of Eon at negative holding potentials and Eoff at positive holding potentials, the linear voltage dependency of the fluorescence magnitude (Figures 2D and 2E, respectively). Indeed, if the electrochromic signals (under the conditions of criteria 3) represented fast conformational movement rather than electric field modulation, these optical components would be described by a Boltzman distribution with voltage, similar to gating charge displacement (e.g., Figures 4A and 4C).

Electric Field Gradient and Structural/ Mechanistic Interpretation

Microscopic and spectroscopic techniques have demonstrated the potential to provide electrostatic detail of integral membrane proteins in artificial bilayers (Philippsen et al., 2002) and soluble polypeptides in solution (Lockhart and Kim, 1992; Park et al., 1999), respectively. However, the electrical information ascertained from these studies essentially represented static systems, as the intrinsically slow temporal response of these methods could not follow dynamic changes in protein structure. With the introduction of site-specific electrochromic detection, electric field profiles of membrane bound proteins in vivo are now readily available at high temporal resolution. In the case of our model system, we resolved an electrostatic field gradient in the loop between the third and fourth transmembrane segments and identified a maximum field strength in the S4—consistent with its role as the primary voltage sensor (Aggarwal and MacKinnon, 1996; Seoh et al., 1996). The large magnitude of the electric field in this region (10×10^5 V/cm from Figure 6) suggests that the hydrophobic core across which the transmembrane voltage falls is compressed by a factor of three (refer to Di-4 field strength, Figure 6) to a dimension of approximately 10 Å. This value represents a lower limit of the real electric field due to the unknown orientation of the fluorophore (see below). It is noteworthy that such a constriction of the hydrophobic portion of the voltage sensor has been inferred from histidine-scanning mutagenesis (Starace and Bezanilla, 2001), and a prediction using continuum electrostatic theory (Islas and Sigworth, 2001) has predicted a constriction of 4 Å.

Since the precise orientation of Di-1-ANEPIA at each site is unknown, a question remains whether the observed electrostatic gradient within the S4 simply reflects a greater tendency toward fluorophore orientation at sites relatively deep within the voltage sensor. We do not believe that is this case due to the following two reasons. (1) If the variation in the electrostatic field was simply a reflection of local environmental constraints, then we would expect that the "most extracellular" residues—278C, 345C, and 425C—would uniformly report small electrostatic fields due to minimal protein packing forces in these regions. However, as shown in Figure 6, 425C experiences an electrostatic field that is equivalent in magnitude to the field near residue 359C in the voltage sensor. (2) Previous work from this laboratory (Cha and Bezanilla, 1998) has demonstrated that environmental constraints near the S4 are diminished with respect to sites in the S3-S4 linker. Therefore, Di-1-ANEPIA is more likely to have a random orientation in the S4 with little tendency to align with the transmembrane electric field. In this scenario, a small rather than large electrostatic field should be detected. Despite the limitations imposed by the unknown fluorophore direction, an orientation effect cannot explain the 3-fold increase in the electrostatic field at site 365C as compared to that in the bilayer. If the field in the voltage sensor was equivalent to that in the membrane, at best, Di-1-ANEPIA would report an electrostatic field of the same magnitude as Di-4-ANEPPS in the bilayer (see below).

Current Limitations and Prospective Improvements

The field strength reported by the Di-1-ANEPIA in the *Xenopus* oocytes represents a lower limit of the actual electric field. Unlike Di-4-ANEPPS, which is engineered to orient normal to the membrane surface to achieve maximal sensitivity to the transmembrane electric field, the precise angle of Di-1-Aneppa (attached to Shaker) relative to the bilayer is unknown. Unfortunately, the highly involuted surface profile of the membrane (Zampighi et al., 1999) complicates the use of polarization measurements to determine the absolute orientation of the fluorophore. If the average direction of Di-1-ANEPIA deviates from the normal of the membrane surface, then the electrochromic shift (and detected electric field) will be diminished as indicated by Equation 1. This angle may be determined from electrochromic measurements of Shaker channels reconstituted into planar lipid bilayers. Notwithstanding, the concordance between our quantitative data (e.g., S4 to charge density distance and bilayer dimension near the voltage sensor) and published results indicates that the Di-1-ANEPIA accurately reports the electric field strength in the ion channel. Despite the current limitation, this site-directed electrochromic technique promises quantitative electrostatic insight toward a vast array of proteins that mediate electrical signaling.

The dimension of the fluorescent probe is the limiting factor for the spatial resolution of this optical technique. Thus, the development of smaller cysteine-reactive electrochromic reagents will impart greater precision to the electrostatic profiles. In addition, an enhancement of this method's optical sensitivity to minute electrical differences is required for the generation of electrostatic maps of proteins characterized by more uniform electrical potential surfaces. Toward this aim, we can utilize narrower spectral band pass filters centered at the maximal slope (Loew et al., 1978) of the "blue edge" of the excitation and emission spectra, respectively. Alternatively, greater sensitivity of the optical signals may be realized with the utilization of ratiometric fluorescence methods (Gross et al., 1994). In this scenario, the opposing effect of "blue" edge relative to "red" edge excitation on the emitted fluorescence would be exploited to maximize the electrochromic signals and simultaneously minimize the background contribution of nonspecific fluorophore populations.

Experimental Procedures

Surface Potential and Charge Density Calculations

The surface potential at the protein-solution interface of Shaker was first calculated by incorporating the observed shift of the Q-V in 70 mM versus 0.5 mM Ca^{2+} into the modified Grahame equation:

$$\sum_{i=1}^{n} C_i[\exp(-z_i F \Psi_0 R^{-1}T^{-1}) - 1] = \sum_{j=1}^{n} C_j[\exp(-z_j F(\Psi_0 + \Delta V)R^{-1}T^{-1}) - 1] \quad (2)$$

where C_i is the bulk concentration and z_i is the valence of the i[th] ionic species in the 0.5 mM Ca^{2+} solution, n is the number of ionic species, C_j is the bulk concentration and z_j is the valence of the j[th] ionic species in the 70 mM Ca^{2+} solution, ψ_0 is the surface potential at the outer membrane, and ΔV is the experimentally measured shift of the Q-V with changes in extracellular calcium (as reflected in Figure 5A). R, T, and F have their typical thermodynamic significance. The surface potential was solved numerically using Maple VII software package (Waterloo Products).

Although the charge density (σ) of Shaker is unlikely to be distributed uniformly, the Grahame equation has been shown to adequately predict the surface potential for σ values more negative than -0.16 e/nm^2 (Peitzsch et al., 1995). Elinder and coworkers have calculated charge densities in the range -0.28 to -0.37 e/nm^2 for members of the Kv1 family of potassium channels and -0.27 e/nm^2 for Shaker in particular (Elinder et al., 1998). The charge density of Shaker was ascertained utilizing the Grahame equation (Gilbert and Ehrenstein, 1969; Grahame, 1947):

$$\sigma_T = \frac{1}{G}\sum_{i=1}^{n} C_i[-z_i F \Psi_0 R^{-1}T^{-1}) - 1]^{1/2}, \quad (3)$$

where G = 2.7 (nm^2/electronic charge) (moles/liter)$^{1/2}$ and the remaining symbols are as defined above.

Debye Length Calculations

The debye length (κ^{-1}) of an aqueous solution represents the distance at which the electrical potential decreases by 1/e. The Debye-Huckel theory posits that κ^{-1} decreases with ionic strength due to the formation of a counter-ion atmosphere that effectively screens each charge. This distance is calculated with the following equation:

$$\kappa^{-1} = \frac{137\text{Å}}{\sqrt{S}}, \quad (4)$$

where S is the ionic strength, specified by

$$S = \sum_i c_i \cdot z_i^2,$$

where c_i is the concentration (mM) and z_i is the valence of the i[th] ion, respectively.

pK_a of Shaker

Extracellular pH perturbates the gating properties of ion channels due to the binding interaction of protons with ionized acidic groups on the protein (Hille, 1991). This modulation of the surface potential is distinct from the screening effect of divalents cations such as calcium (Cukierman et al., 1988; Frankenhaeuser, 1957). The charge density of Shaker is modeled as a homogeneous population of a dissociable acidic group that exhibits negligible proton binding at pH 7.4 (Hille et al., 1975; Ohmori and Yoshii, 1977). The effective charge density at pH 5.5 (σ_E) is diminished relative to the surface charge density at neutral pH (σ_T) as fewer negatively charged acidic groups remain unbound at high proton concentrations. The surface charge density at pH 5.5 (σ_E) is calculated from Equation 3 with the surface potential (ψ_0) equal to the value determined at pH 7.4 ($\psi_0 = -52.1$ mV) and the measured shift of the Q-V with changes in pH ($\Delta V = +21.7$ mV). In this case, the amount of charge neutralized by the protons (assuming 1:1 stoichiometry) is:

$$\sigma_N = \sigma_T - \sigma_E,$$

where $\sigma_N = -0.17$ e/nm^2, $\sigma_T = -0.35$ e/nm^2, and $\sigma_E = -0.18$ e/nm^2.

From the conventions of equilibrium binding, the ratio of the charge density at pH 5.5 (σ_E) and pH 7.4 (σ_T) can be expressed as:

$$\frac{\sigma_E}{\sigma_T} = \frac{1}{(1 + K_a[H^+]_m)}, \quad (5)$$

where $[H^+]_m$ is the proton concentration at the membrane = $[H^+]_{bulk}$ $\exp(-zFVR^{-1}T^{-1})$ and K_a is the equilibrium constant of proton binding. Accordingly, the p$K_a = -\log [K_a]$.

Localization of Di-1-ANEPIA Relative to Shaker

The electrostatic field in the aqueous solution proximal to Shaker is generated by surface charge as described by the one-dimensional Poisson-Boltzmann equation:

$$\frac{d^2\phi(x)}{dx^2} = -\frac{F^2}{RT\epsilon_0\epsilon}\sum_{i=1}^{n} z_i C_i \exp(-z_i F\phi(x)R^{-1}T^{-1}), \quad (6)$$

where $\phi(x)$ is the electrical potential as a function of distance from the channel-solution interface, ϵ_0 is the permitivity of free space, ϵ is the dielectric constant of the medium (water), and C_i is the bulk concentration and z_i is the valence of the i[th] ion in solution. F, R, and T have their usual thermodynamic meanings. The role of the surface charge is to establish a surface potential ($\phi(0)$) that modulates the local concentration of ions based on their valence. In order to determine the electric field, or potential gradient, at a given distance from the protein surface, $d\phi/dx$ is solved by numerical methods. We exploited this mathematical solution of the electrostatic field to localize the electrochromic probe relative to the Shaker surface. The change in electrochromic response (at site 359C) in high and low extracellular calcium (Figure 5D) reflects the perturbation of the local electric field strength. Moreover, the theoretical difference in the electric field magnitude ($d\phi/dx$) in these two ionic conditions was calculated at various distances. By equating the measured change in the electric field to the theoretical difference values, the approximate location of Di-1-ANEPIA relative to the surface charge density was obtained.

Calibration of Di-1-ANEPIA Fluorescence Sensitivity Relative to Di-4-ANEPPS

Given $X(\lambda)$ and $Y(\lambda)$, the excitation and emission spectra, respectively, both normalized to 1 and a bandpass excitation filter from x to $x + B$ (in nm) and a cut-on emission filter starting at y (in nm), the sensitivities are defined as:

$$\frac{dF_x}{d\lambda} = \frac{\frac{d}{d\lambda}\int_x^{x+b} X(z)dz}{\int_x^{x+B} X(z)dz}$$

$$\frac{dF_y}{d\lambda} = \frac{\frac{d}{d\lambda}\int_y^{\infty} Y(z)dz}{\int_y^{\infty} Y(z)dz}$$

where $dF_x/d\lambda$ and $dF_y/d\lambda$ represent the sensitivity of the fluorescence intensity to shifts in the excitation and emission spectra, respectively. For both Di-4-ANEPPS and Di-1-ANEPIA, an excitation bandpass filter between 425 nm and 475 nm was utilized ($x = 425$ nm, $B = 50$ nm). The emission wavelengths differed between the dyes. Experiments with Di-4-ANEPPS employed a 515 nm LP emission filter ($y = 515$), while those with Di-1-ANEPIA employed a 565 nm LP filter ($y = 565$). In the case of both fluorophores, $dF_x/d\lambda$ and $dF_y/d\lambda$ were linear in the limit of small spectral shifts (± 3 nm shifts). The excitation sensitivity of Di-4-ANEPPS was determined to be -0.9% dF/F per nm and the emission sensitivity was $+2.57\%$ dF/F per nm for a net fluorescence sensitivity of 1.67% dF/F per nm. On the other hand, Di-1-ANEPIA yielded a $dF_x/d\lambda$ of -0.13% dF/F per nm and a $dF_y/d\lambda = +2.59\%$ dF/F per nm for a net fluorescence sensitivity of 2.46% dF/F per nm. The net fluorescence sensitivity values ratio between Di-4-ANEPPS and Di-1-ANEPIA was utilized to convert the electrochromic slope factors measured at each site into an electric field using the Di-4-ANEPPS slope as calibration.

Synthesis of Sulfhydryl-Reactive Electrochromic Fluorophores

The starting compound β-[2-(Dimethylamino)-6-naphthyl]-4-vinyl pyridine (I) was prepared from 6-bromo-2-(dimethylamino) naphtha-

lene by the palladium catalyzed Heck coupling procedure (Hassner et al., 1984). A mixture of 210 mg (7.6×10^{-4} mole) of compound I and 400 mg (1.83 mmol) of 3-bromopropylamine hydrobromide in a solution of 6 ml of dry acetonitrile and 3 ml of absolute ethanol was heated at reflux with stirring for a period of 120 hr. All solvents were then removed under reduced pressure on a rotary evaporator, and the resulting residue was taken up in 10 ml of methanol and neutralized with stirring and ice bath cooling by dropwise addition of a solution of 3 ml concentrated ammonium hydroxide in 5 ml of methanol to a final pH of 8–9.5. The neutralized solution was filtered to remove insoluble salts and the solution of amine concentrated to dryness on a rotary evaporator. The crude amine was then taken up in a mixture of methanol and chloroform (1:4) and charged to a column of silica gel 60, packed in chloroform. Unreacted vinyl pyridine starting material was eluted first with chloroform then the product 1-(3-Amino propyl)-4-[β-[2-dimethylamino)-6-naphthyl] vinyl] pyridinium bromide (II) eluted with 50% to 70% methanol in chloroform as a dark red hygroscopic solid, κ_{max} (EtOH) 485 nm. The 200 MHz ^{1}H NMR spectrum (DMSO-d6) was consistent with the structure of compound II.

The synthesis of 1-[3-(β-Maleimidopropionyl) aminopropyl]-4-[β-[2-(dimethylamino)-6-naphthyl] vinyl] pyridinium bromide designated Di-1-ANEPMI (III) required a mixture of 60 mg (1.45×10^{-4} mole) pyridinium propylamine (II) and 40 mg (1.5×10^{-4} mole) β-Maleimidopropionic acid N-hydroxysuccinimide (Sigma Chemical, St. Louis, MO) in 3 ml absolute ethanol and 2 ml methylene chloride to be stirred at ambient temperature under a nitrogen atmosphere. To this mixture was added 2 drops of dry triethylamine and the whole stirred at ambient temperature under nitrogen and protected from light for a total of 212 hr. All solvents were removed under reduced pressure on a rotary evaporator and the resultant dark red residue taken up in 10 ml of 20% methanol in methylene chloride and charged to a column of silica gel packed in methylene chloride. Di-1-ANEPMI was eluted with a mixture of 20% methanol in methylene chloride as a dark red resinous solid. κ_{max} (EtOH) is 484 nm; E_{max} (EtOH) is 670 nm. Thin-layer chromatography (silica gel, methanol-chloroform, 1:4) showed one homogeneous orange-red fluorescent spot, R_f is 0.544. See Figure 8.

1-[3-(Iodoacetyl) amino propyl]-4-[β-(2-dimethylamino)-6-naphthyl] vinyl pyridinium bromide or Di-1-ANEPIA (IV) was synthesized as follows. A mixture of 100 mg (2.42×10^{-4} mole) of pyridinium propyl amine (II) and 102 mg (3.63×10^{-4} mole) of N-hydroxysuccinimide ester of iodoacetic acid (Rector et al., 1978) was added to 4 ml absolute ethanol, 3 ml methylene chloride, and two drops of triethylamine. This was stirred at ambient temperature, under a nitrogen atmosphere, and protected from light for a total of 143 hr. All solvents were then removed under reduced pressure on a rotary evaporator and the dark red residue taken up in 20% methanol in methylene chloride and charged to a column of silica gel 60, packed in methylene chloride. The iodoacetamide product (V) eluted with 20% methanol in methylene chloride as viscous red oil. Thin-layer chromatography (silica gel, methanol-chloroform [1:4]) showed one homogeneous orange fluorescent spot, R_f is 0.564; λ_{max} (EtOH) is 480.5 nm; E_{max} (EtOH) is 713 nm.

The labeling efficiency of Di-1-ANEPIA was found to deteriorate with long storage and was best utilized soon after preparation. Samples were stored at −80°C, protected from air and light.

Channel Constructs, Staining Protocol, and Optical Measurements

All channel mutants were synthesized as described by Starace and coworkers (Starace et al., 1997). Oocytes were stained in 5 μM labeling solution of Di-1-ANEPIA for 40 min, then washed in SOS before recordings. The optical setup has been previously described (Cha and Bezanilla, 1998); a 450DF50 excitation filter, 505LP dichroic, and 515 nm LP filter (Di-4-ANEPPS) or 565 nm LP filter (Di-1-ANEPIA/Di-1-ANEPM)I were utilized for this study.

Acknowledgments

We thank Dr. Michael Green for his initial encouragement to perform these measurements. We are indebted to Jose Luis Vazquez-Ibar for assistance in obtaining fluorescence spectral data in oocytes. This work was supported by a NIH predoctoral fellowship to O.K.A. (1 F31 GM20596-03) and NIH grants to L.M.L. (GM35063) and F.B. (GM30376). An additional source of funding was provided by MURI/ONR grant N00014-99-1-0717 to L.M.L.

Received: May 13, 2002
Revised: November 18, 2002

References

Aggarwal, S.K., and MacKinnon, R. (1996). Contribution of the S4 segment to gating charge in the Shaker K+ channel. Neuron *16*, 1169–1177.

Baker, O.S., Larsson, H.P., Mannuzzu, L.M., and Isacoff, E.Y. (1998). Three transmembrane conformations and sequence-dependent displacement of the S4 domain in shaker K+ channel gating. Neuron *20*, 1283–1294.

Bedlack, R.S., Jr., Wei, M.D., Fox, S.H., Gross, E., and Loew, L.M. (1994). Distinct electric potentials in soma and neurite membranes. Neuron *13*, 1187–1193.

Bezanilla, F. (2000). The voltage sensor in voltage-dependent ion channels. Physiol. Rev. *80*, 555–592.

Brink, F. (1954). The role of calcium ions in neural processes. Pharmacol. Rev. *6*, 243–298.

Canepari, M., Campani, M., Spadavecchia, L., and Torre, V. (1996). CCD imaging of the electrical activity in the leech nervous system. Eur. Biophys. J. *24*, 359–370.

Carnay, L.D., and Barry, W.H. (1969). Turbidity, birefringence, and fluorescence changes in skeletal muscle coincident with the action potential. Science *165*, 608–609.

Cha, A., and Bezanilla, F. (1997). Characterizing voltage-dependent conformational changes in the Shaker K+ channel with fluorescence. Neuron *19*, 1127–1140.

Cha, A., and Bezanilla, F. (1998). Structural implications of fluorescence quenching in the Shaker K+ channel. J. Gen. Physiol. *112*, 391–408.

Cha, A., Snyder, G.E., Selvin, P.R., and Bezanilla, F. (1999). Atomic scale movement of the voltage-sensing region in a potassium channel measured via spectroscopy. Nature *402*, 809–813.

Cohen, L.B., Salzberg, B.M., Davila, H.V., Ross, W.N., Landowne, D., Waggoner, A.S., and Wang, C.H. (1974). Changes in axon fluorescence during activity: molecular probes of membrane potential. J. Membr. Biol. *19*, 1–36.

Cukierman, S., Zinkand, W.C., French, R.J., and Krueger, B.K. (1988). Effects of membrane surface charge and calcium on the gating of rat brain sodium channels in planar bilayers. J. Gen. Physiol. *92*, 431–447.

Doyle, D.A., Cabral, J.M., Pfuetzner, R.A., Kuo, A.L., Gulbis, J.M., Cohen, S.L., Chait, B.T., and MacKinnon, R. (1998). The structure of the potassium channel: molecular basis of K+ conduction and selectivity. Science *280*, 69–77.

Elinder, F., and Arhem, P. (1999). Role of individual surface charges of voltage-gated K channels. Biophys. J. *77*, 1358–1362.

Elinder, F., Liu, Y., and Arhem, P. (1998). Divalent cation effects on the Shaker K channel suggest a pentapeptide sequence as determinant of functional surface charge density. J. Membr. Biol. *165*, 183–189.

Frankenhaeuser, B., and Hodgkin, A.L. (1957). The action of calcium on the electrical properties of squid axons. J. Physiol. (London) *137*, 218–244.

Gilbert, D.L., and Ehrenstein, G. (1969). Effect of divalent cations on potassium conductance of squid axons: determination of surface charge. Biophys. J. *9*, 447–463.

Glauner, K.S., Mannuzzu, L.M., Gandhi, C.S., and Isacoff, E.Y. (1999). Spectroscopic mapping of voltage sensor movement in the Shaker potassium channel. Nature *402*, 813–817.

Grahame, D.C. (1947). The electrical double layer and the theory of electrocapillarity. Chem. Rev. *41*, 441.

Green, W.N., and Andersen, O.S. (1991). Surface charges and ion channel function. Annu. Rev. Physiol. *53*, 341–359.

Gross, E., Bedlack, R.S., Jr., and Loew, L.M. (1994). Dual-wavelength ratiometric fluorescence measurement of the membrane dipole potential. Biophys. J. *67*, 208–216.

Hassner, A., Birnbaum, D., and Loew, L.M. (1984). Charge shift probes of membrane potential. Synthesis. J. Org. Chem. *49*, 2546–2551.

Hille, B. (1991). Modifiers of Gating. In Ionic Channels of Excitable Membranes (Sunderland, MA: Sinauer Associates), pp. 445–503.

Hille, B., Woodhull, A.M., and Shapiro, B.I. (1975). Negative surface charge near sodium channels of nerve: divalent ions, monovalent ions, and pH. Philos. Trans. R. Soc. Lond. B Biol. Sci. *270*, 301–318.

Hodgkin, A.L., and Huxley, A.F. (1952). A quantitative description of membrane current and its application to conduction and excitation in nerve. J. Physiol. *117*, 500–544.

Honig, B., and Nicholls, A. (1995). Classical electrostatics in biology and chemistry. Science *268*, 1144–1149.

Islas, L.D., and Sigworth, F.J. (2001). Electrostatics and the gating pore of Shaker potassium channels. J. Gen. Physiol. *117*, 69–89.

Ji, S., Weiss, J.N., and Langer, G.A. (1993). Modulation of voltage-dependent sodium and potassium currents by charged amphiphiles in cardiac ventricular myocytes. Effects via modification of surface potential. J. Gen. Physiol. *101*, 355–375.

Lakowicz, J.R. (1999). Introduction to Fluorescence. In Principles of Fluorescence Spectroscopy (New York: Kluwer Academic/Plenum Publishers), pp. 1–23.

Larsson, H.P., Baker, O.S., Dhillon, D.S., and Isacoff, E.Y. (1996). Transmembrane movement of the shaker K+ channel S4. Neuron *16*, 387–397.

Lockhart, D.J., and Kim, P.S. (1992). Internal stark effect measurement of the electric field at the amino terminus of an alpha helix. Science *257*, 947–951.

Loew, L.M. (1982). Design and characterization of electrochromic membrane probes. J. Biochem. Biophys. Methods *6*, 243–260.

Loew, L.M., Bonneville, G.W., and Surow, J. (1978). Charge shift optical probes of membrane potential. Theory Biochemistry *17*, 4065–4071.

Loew, L.M., Cohen, L.B., Dix, J., Fluhler, E.N., Montana, V., Salama, G., and Wu, J.Y. (1992). A naphthyl analog of the aminostyryl pyridinium class of potentiometric membrane dyes shows consistent sensitivity in a variety of tissue, cell, and model membrane preparations. J. Membr. Biol. *130*, 1–10.

Mannuzzu, L.M., Moronne, M.M., and Isacoff, E.Y. (1996). Direct physical measure of conformational rearrangement underlying potassium channel gating. Science *271*, 213–216.

Meister, A. (1995). Thiol/Disulfide Exchange. In Biothiols Part A Monothiols and Dithiols, Protein Thiols, and Thiyl Radicals, L. Packer, ed. (San Diego: Academic Press, Inc.), pp. 3–28.

Ohmori, H., and Yoshii, M. (1977). Surface potential reflected in both gating and permeation mechanisms of sodium and calcium channels of the tunicate egg cell membrane. J. Physiol. *267*, 429–463.

Park, E.S., Anderews, S., Hu, R.B., and Boxer, S.G. (1999). Vibrational stark spectroscopy in proteins: a probe and calibration for electrostatic fields. J. Phys. Chem. B *103*, 9813–9817.

Peitzsch, R.M., Eisenberg, M., Sharp, K.A., and McLaughlin, S. (1995). Calculations of the electrostatic potential adjacent to model phospholipid bilayers. Biophys. J. *68*, 729–738.

Perozo, E., MacKinnon, R., Bezanilla, F., and Stefani, E. (1993). Gating currents from a nonconducting mutant reveal open-closed conformations in Shaker K+ channels. Neuron *11*, 353–358.

Philippsen, A., Im, W.P., Engel, A., Schirmer, T., Roux, B., and Muller, D.J. (2002). Imaging the electrostatic potential of transmembrane channels: atomic probe microscopy of OmpF porin. Biophys. J. *82*, 1667–1676.

Rector, E.S., Schwenk, R.J., Tse, K.S., and Sehon, A.H. (1978). A method for the preparation of protein-protein conjugates of predetermined composition. J. Immunol. Methods *24*, 321–336.

Rohr, S., and Salzberg, B.M. (1994). Multiple site optical recording of transmembrane voltage (MSORTV) in patterned growth heart cell cultures: assessing electrical behavior, with microsecond resolution, on a cellular and subcellular scale. Biophys. J. *67*, 1301–1315.

Sadler, S.E. (2001). Low-density caveolae-like membrane from *Xenopus laevis* oocytes is enriched in Ras. J. Cell. Biochem. *83*, 21–32.

Seoh, S.A., Sigg, D., Papazian, D.M., and Bezanilla, F. (1996). Voltage-sensing residues in the S2 and S4 segments of the Shaker K+ channel. Neuron *16*, 1159–1167.

Sorensen, J.B., Cha, A., Latorre, R., Rosenman, E., and Bezanilla, F. (2000). Deletion of the S3-S4 linker in the Shaker potassium channel reveals two quenching groups near the outside of S4. J. Gen. Physiol. *115*, 209–222.

Starace, D.M., and Bezanilla, F. (2001). Histidine scanning mutagenesis of basic residues of the S4 segment of the shaker K+ channel. J. Gen. Physiol. *117*, 469–490.

Starace, D.M., Stefani, E., and Bezanilla, F. (1997). Voltage-dependent proton transport by the voltage sensor of the Shaker K+ channel. Neuron *19*, 1319–1327.

Tasaki, I., Watanabe, A., Sandlin, R., and Carnay, L. (1968). Changes in fluorescence, turbidity, and birefringence associated with nerve excitation. Proc. Natl. Acad. Sci. USA *61*, 883–888.

Waggoner, A.S., and Grinvald, A. (1977). Mechanisms of rapid optical changes of potential sensitive dyes. Ann. N Y Acad. Sci. *303*, 217–241.

Yuste, R., Tank, D.W., and Kleinfeld, D. (1997). Functional study of the rat cortical microcircuitry with voltage-sensitive dye imaging of neocortical slices. Cereb. Cortex *7*, 546–558.

Zampighi, G.A., Loo, D.D., Kreman, M., Eskandari, S., and Wright, E.M. (1999). Functional and morphological correlates of connexin50 expressed in *Xenopus laevis* oocytes. J. Gen. Physiol. *113*, 507–524.

Zhang, J., Loew, L.M., and Davidson, R.M. (1996). Faster voltage-dependent activation of Na^+ channels in growth cones versus somata of neuroblastoma N1E–115 cells. Biophys. J. *71*, 2501–2508.

Zhang, J., Davidson, R.M., Wei, M.D., and Loew, L.M. (1998). Membrane electric properties by combined patch clamp and fluorescence ratio imaging in single neurons. Biophys. J. *74*, 48–53.